X-Ray Diffraction Characterisation of Nanoparticle Size and Shape Distributions:— Application to Bimodal Distributions

Nicholas Armstrong[a,1], Walter Kalceff [a], James P. Cline[b], John Bonevich[b], Peter A. Lynch[a], Chiu C. Tang[c] and Steve P. Thompson[c]

[a] *University of Technology Sydney, PO Box 123, Broadway NSW 2007 AUSTRALIA.*
[b] *National Institute of Standards and Technology, Gaithersburg, MD 20899, USA.*
[c] *CLRC Daresbury Laboratory, Daresbury, WA4 4AD, UK*

Abstract We present a novel Bayesian/Maximum Entropy method to detect and resolve the modal characteristics of size distributions from x-ray diffraction line profiles. To our knowledge, none of the existing alternative methods are capable of extracting this information from experimental data.

1. Introduction

The mass production of functional nanoparticles will be a key element in the development of smart appliances and technologies [1], requiring both the ability to grow particles in various shapes to serve as a basis for more complex structures [1–4], and relatively fast experimental/analytical techniques for characterising microstructural properties (e.g. shape, size distribution, and internal defect content).

Although recent advances in x-ray line profile analysis already provide the means for obtaining microstructural information in an industrial environment [5–10], the development of a NIST particle size Standard Reference Material (SRM 1979) will allow routine assessment of analytical and experimental methods for characterising nanoparticles. The SRM will consist of two materials, viz. cerium oxide (10–40 nm) and zinc oxide (40–60 nm), with spherical and cylindrical morphologies, respectively. The range of sizes and shapes will allow for a variety of methods and models to be applied to obtain an XRD "bulk" picture of materials. Bayesian/Maximum Entropy methods have been developed to analyse particle shape and size distribution information from line profile data [11, 5]; these methods will be used to certify the SRM. Here we present an overview of the application of the method for detecting and resolving bimodal size distributions from x-ray line profile data.

2. Outline of Theory & Results

An observed XRD line profile is made up of a number of broadening contributions, including instrumental effects (diffractometer), specimen effects, background effects and statistical noise. Assuming specimen broadening is only defined by size/shape effects, the observed profile can be expressed as a function of the scattering vector s by

$$g(s) = \int_0^\infty K(s,\mathbf{D})P(\mathbf{D})d\mathbf{D} + b(s) + n(s), \quad \forall s \in [-\infty,\infty] \tag{1}$$

where $K(s,\mathbf{D})$ combines the scattering kernels of the crystallites and the instrument (see eqns. 8.7–13 in [5]) and $P(\mathbf{D})$ defines the size distribution of the crystallites, where $\mathbf{D} = \{D_1, D_2, D_3\}$ corresponds to the crystallite dimensions. Finding $P(\mathbf{D})$ from (1) requires solving an inverse problem, but because $K(s,\mathbf{D})$ is generally ill-conditioned many possible solutions may fit the observed data. $P(\mathbf{D})$ is of course expected to correspond to the distribution determined from direct observations, such as TEM.

[1] E-mail: Nicholas.Armstrong@uts.edu.au

The problem of determining the modal characteristics of a size distribution from the line profile data is essentially a selection problem between competing models [12]. Using Bayes' theorem, we can state the *a posteriori* probability that the size distributions is bimodal, say model M_1, defined by two lognormal distribution functions with modes $D_{01,M1}$, and $D_{02,M2}$, lognormal standard deviations, $\sigma_{01,M2}$ and $\sigma_{02,M2}$, and a relative mixture η of the two (with $0 \le \eta \le 1$) as

$$\Pr(M_1 \mid g, \sigma, I) = \Pr(M_1, I) \Pr(g \mid M_1, \sigma, I) / \Pr(g \mid \sigma, I) \tag{2}$$

where g defines the observed diffraction profile given in (1); σ is the standard deviation of the intensity, which can be approximated as $\sigma \approx \sqrt{g}$; and I is any information we have about the problem and distributions. $\Pr(M_1, I)$ defines an *a priori* probability for M_1, and $\Pr(g \mid M_1, \sigma, I)$ is the integrated likelihood probability distribution for M_1 such that $\Pr(g \mid M_1, \sigma, I) = \int \mathrm{d}\vec{\xi} \Pr(\vec{\xi}, g \mid M_1, \sigma, I)$, with $\Pr(\vec{\xi}, g \mid M_1, \sigma, I)$ defining the joint probability for the parameters, $\vec{\xi} = \{D_{01,M1}, D_{02,M1}, \sigma_{01,M1}, \sigma_{02,M1}, \eta\}$ and g. The denominator in (2) is defined as $\Pr(g \mid \sigma, I) = \sum_{i=1}^{N} \Pr(M_i, g \mid \sigma, I)$ for N models. Similarly, we can define a second model M_2 which assumes that the size distribution is mono-modal, defined by a lognormal distribution function with parameters $D_{01,M2}$ and $\sigma_{02,M2}$. The model which produces the greatest probability is clearly "best" and can serve in the MaxEnt approach as the *a priori* model [5].

Using the procedure outlined in [11], simulated diffraction data for the 200 peak was generated for spherical gold nanoparticles with a lognormal bimodal size distribution. Figure 1(a) shows the simulated observed profile, instrument profile and estimated background level. The instrument profile was modelled on the settings given in Fig. 7 of [11]. Figure 1(b) shows the MaxEnt distribution for a uniform model which assumes the size distribution has no structure for all values of $D \in [0, 85\ \mathrm{nm}]$. The range of D can be determined from the Fourier coefficients of the specimen profile [11, 5]. The MaxEnt solution for this model indicates that there is structure in the data and warrants further investigation. At this point, the model selection theory outlined above is used to select between the two possible models: M_1 predicts the size distribution is bimodal defined by a lognormal distribution function; M_2 predicts a monomodal distribution with a lognormal function. A Markov Chain Monte Carlo (MCMC) method described in [5] was used to determine the optimum parameters and probabilities for each model (also see [13]). The MCMC method used 6.0×10^4 samples in each case, determined by trial and error to produce representative statistics for each model. Figure 1(c) shows the two models compared with the theoretical distribution. The fit between M_1 and the theoretical distribution is very good, while for M_2 the MCMC method has tried to compensate by producing a monomodal distribution with a greater average particle size in order to fit the observed data. The probabilities determined for each model were: $\log_{10}[\Pr(M_1 \mid g, \sigma)] \approx -245.59$ and $\log_{10}[\Pr(M_2 \mid g, \sigma)] \approx -252.84$. This application of Bayesian model selection confirms the results in Figure 1(c). Although the probabilities are very small, they take into account the variance of the diffraction data and uncertainty in the estimated background level, and have been normalised. Using M_1 as the *a priori* model in the MaxEnt method, further refinement and full quantitative determination of $P(D)$ can be achieved. This is shown in Figure 1(d), with the error-bars arising from uncertainties in the counting statistics and background estimation. Figure 1(d) shows the effectiveness of the Bayesian/MaxEnt method in determining a $P(\mathbf{D})$ with bimodal properties.

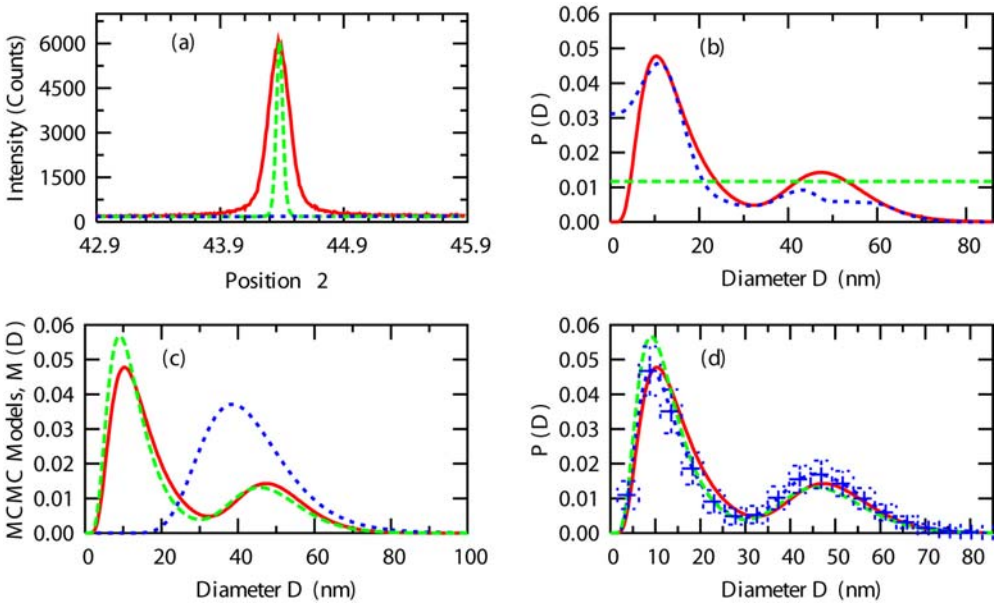

Fig. 1. Simulated diffraction data, MCMC & Bayesian size distribution results for Au spherical nanocrystallites. (a) The simulated "observed" line profile (red), instrument profile (green) and estimate background level (blue). (b) Theoretical bimodal size distribution (red) and MaxEnt solution (blue) for a uniform model (green). (c) Theoretical bimodal size distribution (red), the MCMC models: monomodal distribution (blue) and bimodal distribution (green); (d) Theoretical bimodal size distribution (red) and MaxEnt solution for a bimodal model (blue + error-bars); the MCMC bimodal model (green) from (c) is also shown.

3. Conclusion

The Bayesian/MaxEnt method outlined here has demonstrated it can detect and resolve bimodal particle distributions from analysis of their XRD diffraction patterns. This has been achieved through Bayesian model selection from which an *a priori* model was determined.

References

[1] L. Manna, D. J. Milliron, A. Meisel, E. C. Scher, and A. P. Alivisatos. *Nature Materials*, 2: 382 (2003).

[2] P. L. Gai and M. A. Harmer. *NanoLett.*, 2 (7): 771 (2002).

[3] M. Hu, X.Wang, G. V. Hartland, P. Mulvaney, J. P. Juste, and J. E. Sader. *J. Am. Chem. Soc.*, 125: 14925 (2003).

[4] D. Wang and C. M. Lieber. *Nature Materials*, 2: 355 (2003).

[5] N. Armstrong, W. Kalceff, J. P. Cline, and J. Bonevich. in *Diffraction analysis of the microstructure of materials*, eds. E. J. Mittemeijer & P. Scardi (Springer-Verlag, Berlin 2003), 187.

[6] C. E. Krill and R. Birringer. *Phil. Mag.*, A77(3):621 (1998).

[7] J. I. Langford, D. Lou¨er, and P. Scardi. *J. Appl. Cryst.*, 33: 964 (2000).

[8] P. Scardi and M. Leoni. *Acta Cryst.*, A57:604 (2001).

[9] Scardi and M. Leoni. *Acta Cryst.*, A58: 190 (2002).

[10] T. Ungar, J. Gubicza, G. Ribarik, and A. Borbely. *J. Appl. Cryst.*, 34: 298 (2001).

[11] N. Armstrong, W. Kalceff, J. P. Cline, and J. Bonevich. "Bayesian inference of nanoparticle broadened x-ray line profiles". *J. Res. Nat. Inst. Stand. Techn.*, 108 (5): in press; also see URL:http://xxx.lanl.gov/physics/0305018, 2003.

[12] D. S. Sivia. *Data Analysis: A Bayesian Tutorial* (Oxford Science Pub., Oxford, 1996).

[13] J. J. K. O'Ruanaidh and W. J. Fitzgerald. *Numerical Bayesian methods applied to signal processing* (Springer, New York, 1996).